Available online at www.sciencedirect.com
ScienceDirect
Tectonophysics xx (2008) xxx–xxx
TECTONOPHYSICS
www.elsevier.com/locate/tecto

Quaternary fault segmentation and interaction in the epicentral area of the 1561 earthquake (Mw = 6.4), Vallo di Diano, southern Apennines, Italy

V. Spina [a,*], E. Tondi [a], P. Galli [b], S. Mazzoli [c], G. Cello [a]

[a] Dipartimento di Scienze della Terra, Università di Camerino, Via Gentile III da Varano, 62032 Camerino (MC), Italy
[b] Dipartimento della Protezione Civile, Ufficio Servizio Sismico Nazionale, Via di Vitorchiano, Roma, Italy
[c] Dipartimento Scienze della Terra, Università di Napoli 'Federico II', Largo San Marcellino 10, 80138 Napoli, Italy

Received 7 October 2006; accepted 5 June 2007

Abstract

The main structural characteristics of the Caggiano and Polla faults, exposed in the epicentral area of the 1561 earthquake (Mw = 6.4), southern Italy, have been investigated in detail to assess their spatial and temporal properties, and to evaluate their seismogenic potential. These right stepping normal faults show an overlap of about 7 km and an across strike separation of about 4 km. The geometric relationships between the Caggiano and Polla faults, but also the displacement distribution along each fault, demonstrate that they have been strongly interacting throughout the Pleistocene. Nevertheless, geological evidence of Holocene tectonic activity was mainly recognized along the Caggiano Fault (faulted late glacial deposits) and in the southernmost part of the Polla Fault (faulted deposits of probably Late Pleistocene age). This suggests that the Caggiano Fault can be considered as the most tectonically active fault in the Vallo di Diano Fault System. By calculating Coulomb stress changes, we have constrained modes of mechanical interactions between the two faults in a scenario compatible with the 1561 earthquake. This approach allows us to argue that both the Caggiano and the Polla Faults are probably linked at depth, and part of the same seismogenic structure which may be potentially responsible for composite ruptures with magnitude ≥ 6.5.

Keywords: Active tectonics; earthquake faults; intermountain basins; structural analysis

1. Introduction

Fault interaction processes strongly control the seismic hazard of a region. It is well know that pre-linkage fault interaction combined with post-linkage displacement readjustment influences the measured displacement–length ratio (Peacock and Sanderson, 1991; Cartwright et al., 1995; Willemse et al., 1996; Willemse, 1997; Gupta and Scholz, 2000; Cowie and Roberts, 2001; Roberts et al., 2004), while the mean recurrence interval tends to decrease as slip-rate increases. The proposed mechanism explaining how displacement profile re-adjustment occurs during growth by linkage (Cowie, 1998) is based on the observation that during earthquakes the stress level increases along fault strike. The increasing stress level can also determine the distortion of the displacement profile (Gupta and Scholz, 2000) and can advance the timing of future earthquakes on neighbouring along-strike faults (Hodgkinson et al., 1996). In particular, Cowie (1998) demonstrates that along-strike neighboring faults may interact through their stress fields to generate larger earthquakes.

Therefore, to determine the seismic hazard of a region is fundamental to understand if neighbouring along-strike faults interact. For example, the strongest historical earthquakes along the Italian peninsula were generated by the activation, almost simultaneously, of more than one along-strike seismogenic fault (e.g. the 1703 Norcia-L'Aquila earthquake, Cello et al., 1997, Galadini and Galli, 2000; Tondi, 2000; the 1980 Irpinia earthquake, Pantosti and Valensise 1990, Porfido et al., 2002; the 1857 Basilicata earthquake, Benedetti et al., 1998; Cello et al., 2003).

The integration of geological, morphotectonic and geophysical information appears to be fundamental for the interpretation of the subsurface structure of fault zones and for understanding the

* Corresponding author. Now at Fugro Robertson Ltd., Llandudno, UK.
E-mail address: vincenzo.spina@fugro-robertson.com (V. Spina).

0040-1951/$ - see front matter © 2008 Elsevier B.V. All rights reserved.
doi:10.1016/j.tecto.2007.06.012

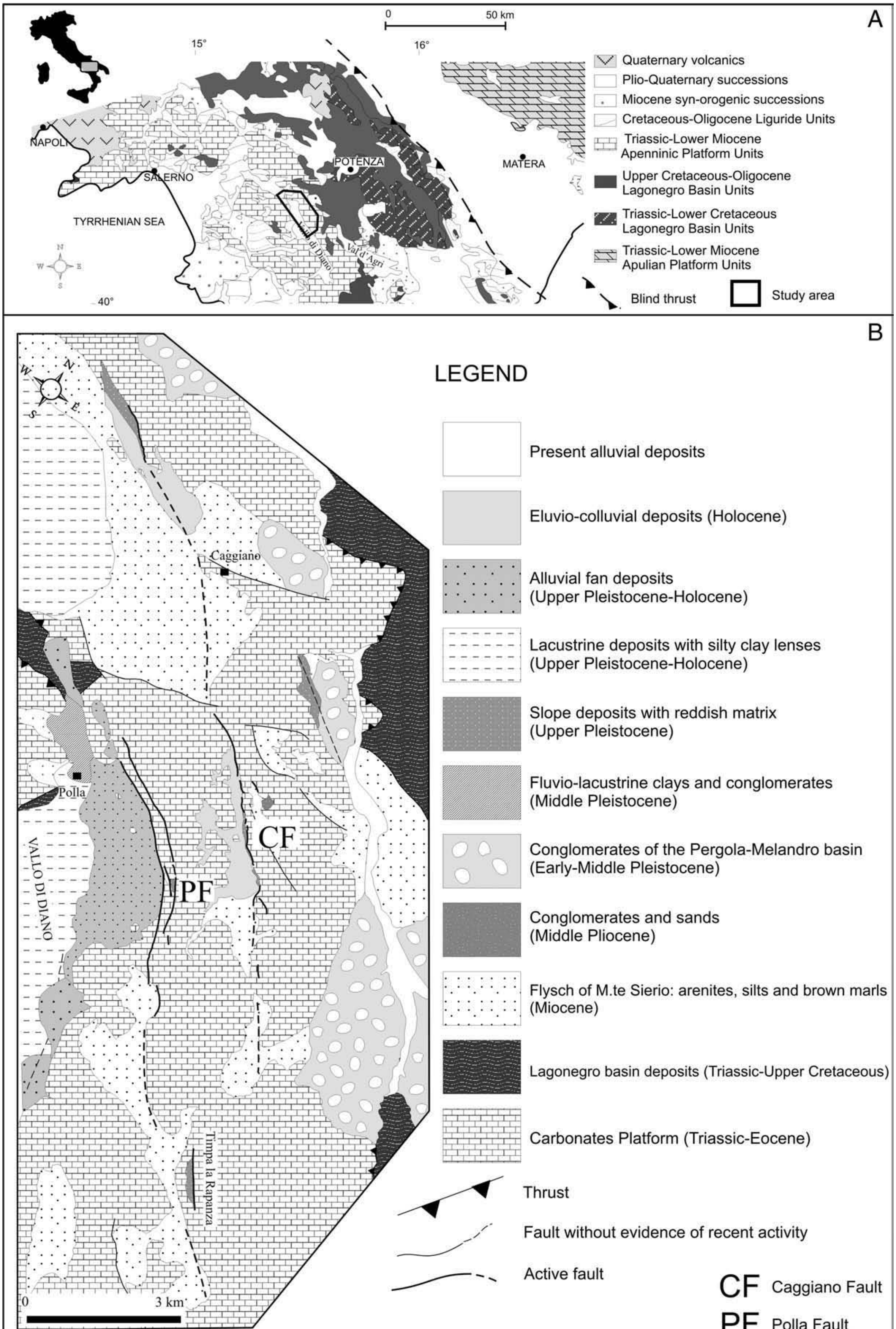

Fig. 1. (A) Simplified geological map of the southern Apennines. (B) Geological map of the northeastern sector of the Vallo di Diano Basin.

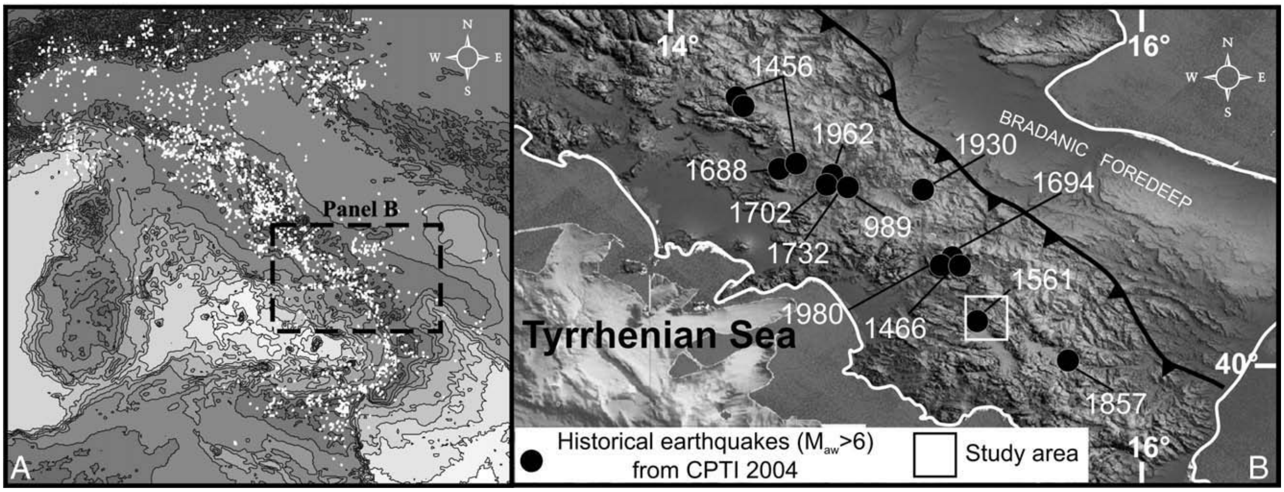

Fig. 2. (A) Location of the historical earthquakes in the Italian peninsula (data from CPTI, 2004). (B) Principal historical earthquakes (Mw > 6) in the southern Apennines (data from CPTI, 2004).

related fault growth processes. This, in turn, is fundamental for any seismotectonic modelling and assessment of earthquake-related hazards.

In this work, we investigate the main structural characteristics of the Caggiano and Polla faults (two active fault segments belonging to the Vallo di Diano Fault System in southern Italy, DIFS in Cello et al., 2003). The goal is the evaluation of their modes of interaction, and the definition of the seismic hazard associated with these structures, which were probably re-activated (Cello et al., 2003) during both the 1561 (Mw = 6.4) and the 1857 (Mw = 6.9) earthquakes (CPTI, 2004).

2. Geological setting

The Southern Apennines are a NE-vergent fold-and-thrust belt, which evolved within the framework of the convergent motion between the Afro-Adriatic and European plates since Late Cretaceous times (Butler et al., 2004; Cello et al., 1989; Dewey et al., 1989; Mazzoli and Helman, 1994; Rosenbaum et al., 2002). Except for the remnants of the ophiolite-bearing Liguride Units that occur on top of the thrust pile, outcropping units consist of Mesozoic and Cenozoic rocks derived from the sedimentary cover of the of the Afro-Adriatic continental margin. These include both Mesozoic–Tertiary shallow-water-to-slope sediments of the so-called 'Apennines' carbonate platforms and pelagic (Lagonegro Basin) successions, as well as unconformable Miocene siliciclastic deposits (e.g., Mostardini and Merlini, 1986; Sgrosso, 1998; Cello and Mazzoli, 1999, Mazzoli et al., 2001).

Neogene thrusting in the southern Apennines was accompanied by back-arc extension and sea-floor spreading in the southern Tyrrhenian Sea (e.g., Kastens et al., 1988, Fig. 1). According to several Authors (e.g., Cello et al., 1982; Cinque et al., 1993; Hippolyte et al., 1994; Cello and Mazzoli, 1999), around the Early-Middle Pleistocene boundary (*ca.* 0.8 Ma), the SW–NE shortening ceased in the frontal parts of the southern Apennines and a new tectonic regime was established in the chain and adjacent foothills. The structures related to this new regime consist of extensional and transcurrent faults postdating and dissecting the thrust belt (e.g., Cello et al., 1982, 2003; Butler et al., 2004).

The Vallo di Diano is a Plio-Quaternary basin filled with fluvio-lacustrine fan and slope deposits (Ascione et al., 1992; Cinque et al., 1993; Giano et al., 2000) (Fig. 1B). This basin is bounded to the west by the Monti Alburni Ridge, which consist of Cretaceous to Palaeogene Apenninic platform carbonates (D'Argenio et al., 1973). To the east, it is limited by the Monti della Maddalena Ridge, which is made up of Mesozoic–Palaeogene

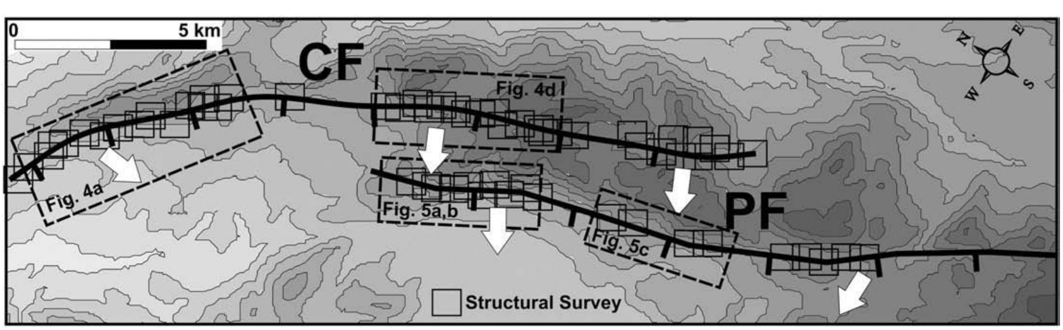

Fig. 3. Topographic contour map of the study area. Two major NW – SE oriented normal faults, CF and PF, crop out along the eastern border of the Vallo di Diano Basin. Along faults 70 stations of structural survey were carried out in order to characterize kinematic properties of the faults. Black arrows show main kinematics observed in the different sector of the faults. Boxes show locations of photographic documentation for each fault.

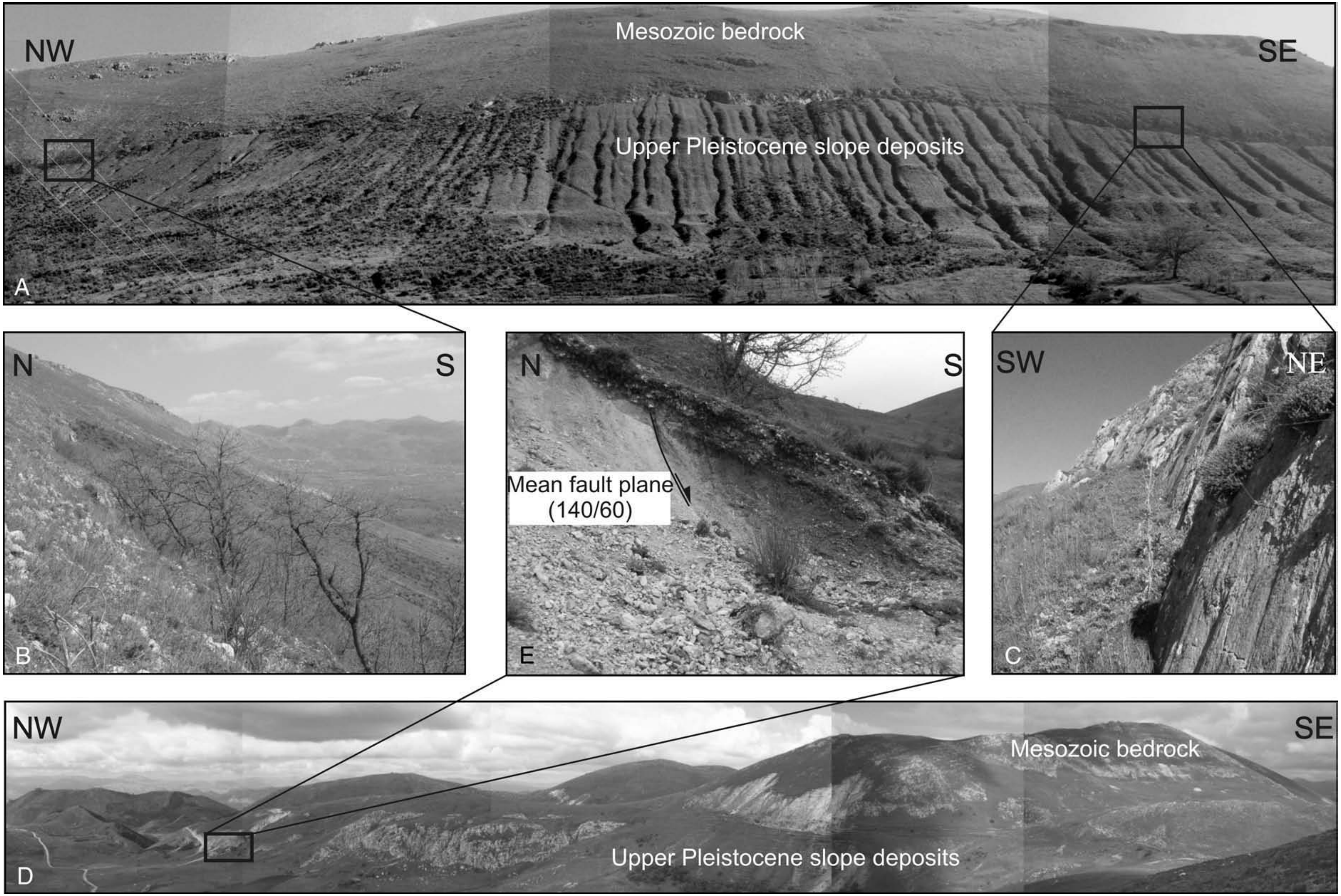

Fig. 4. Morphotectonic features of the CF. (A, B and C) in the northernmost tip zone the fault scarp brings into contact Meso-Cenozoic carbonates with Upper Pleistocene slope deposits. In the southern sector this fault is characterized by a complex fault array (D) and offset eluvio–colluvial Upper Pleistocene and Holocene deposits (E).

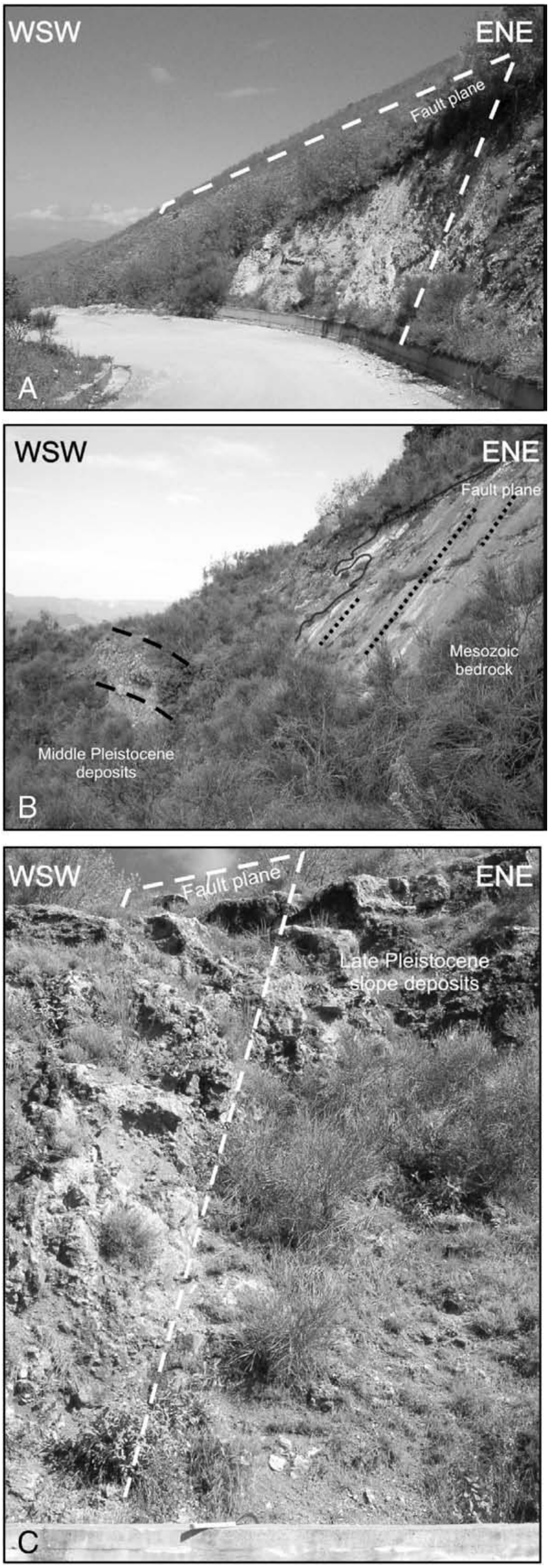

Fig. 5. Morphotectonic features of the PF. (A) Main fault plane of the PF in Meso-Cenozoic carbonates. (B) The same structure affects also Middle Pleistocene slope deposits determining their back tilting against the smoothed fault plane. (C) The PF displaces also Middle–Upper Pleistocene deposits.

successions, that include both Apenninic carbonate platform units and Lagonegro Basin units (Scandone and Bonardi, 1968). The general architecture of the basin depicts a half-graben structure, bounded by a major NW–SE striking fault to the east (Ascione et al., 1992; Cinque et al., 1993; Catalano et al., 2004).

3. Seismotectonic background

Within the instrumental time windows, the study area of Italy, is affected by several moderate earthquakes (Mw < 6) that depict a seismic belt trending roughly NW–SE (Fig. 2A). However, in the last millennium many events with Mw > 6 struck the southern sector of the Italian peninsula (Fig. 2B). These occurred mainly along the axial zone of the Apennines, and have been related to normal, transtensional, and/or strike-slip faults (Pantosti & Valensise, 1990; Montone et al., 1999; Cello et al., 2003; Galli et al., 2006). In the last centuries, the most destructive events in the area were: the 1561 earthquake (Mw = 6.4, CPTI, 2004), the 1857 earthquake (Mw = 6.9, CPTI, 2004), and the 1980 Irpinia earthquake (Mw = 6.9, CPTI, 2004).

Of particular interest are the macroseismic fields reconstructed for the 1857 and the 1561 earthquakes, which struck the Vallo di Diano and the Val d'Agri areas, respectively (Boschi et al., 1997). In particular, the 1857 earthquake was characterized by an epicentral zone elongated in a NW–SE direction for about 60 km. Within this area, there are several faults belonging to two different fault systems (i.e. the Vallo di Diano Fault System: DIFS, and the Val d'Agri Fault System: VAFS; see Cello et al., 2003), both showing evidences of recent tectonic activity. In between, the roughly north–south trending calcareous ridge of the Monti della Maddalena represents a topographic high separating the two basin areas. Branno et al. (1983) propose that the isoseismal field related to the 1857 event could be due to the cumulative effects of two main shocks, one located in the Vallo di Diano and the other in the Val d'Agri area. Cello et al. (2003) and Galli et al. (2006) suggested that this seismogenic zone is characterized by a twofold behaviour, as it is capable of causing: (i) large earthquakes ($M \geq 7.0$) as a result of composite ruptures on both fault systems, and (ii) medium-size earthquakes ($M = 6$–6.5), in case only one of the two fault systems ruptures.

This mode of seismic energy release is typical also of other areas in peninsular Italy. The strongest historical earthquakes in the Italian peninsula (i.e. the 1703 Norcia-L'Aquila earthquake, see Cello et al., 1997; Tondi, 2000; Galadini & Galli, 2000; the 1980 Irpinia earthquake, see Pantosti and Valensise 1990 and Porfido et al., 2002; the 1857 Basilicata earthquake, see Benedetti et al., 1998 and Cello et al., 2003) were, in fact, all accompainied by multiple fault reactivation.

4. Structural analysis

Detailed structural data were collected on two active faults belonging to the Vallo di Diano Fault System: the Caggiano and Polla Faults (Figs. 1 and 3). The Caggiano Fault (CF) is a 17 km-long structure cutting across different rock units of Mesozoic to Holocene age (Cello et al., 2003; Galli and Bosi,

Please cite this article as: Spina, V., et al., Quaternary fault segmentation and interaction in the epicentral area of the 1561 earthquake (Mw = 6.4), Vallo di Diano, southern Apennines, Italy, Tectonophysics (2008), doi:10.1016/j.tecto.2007.06.012

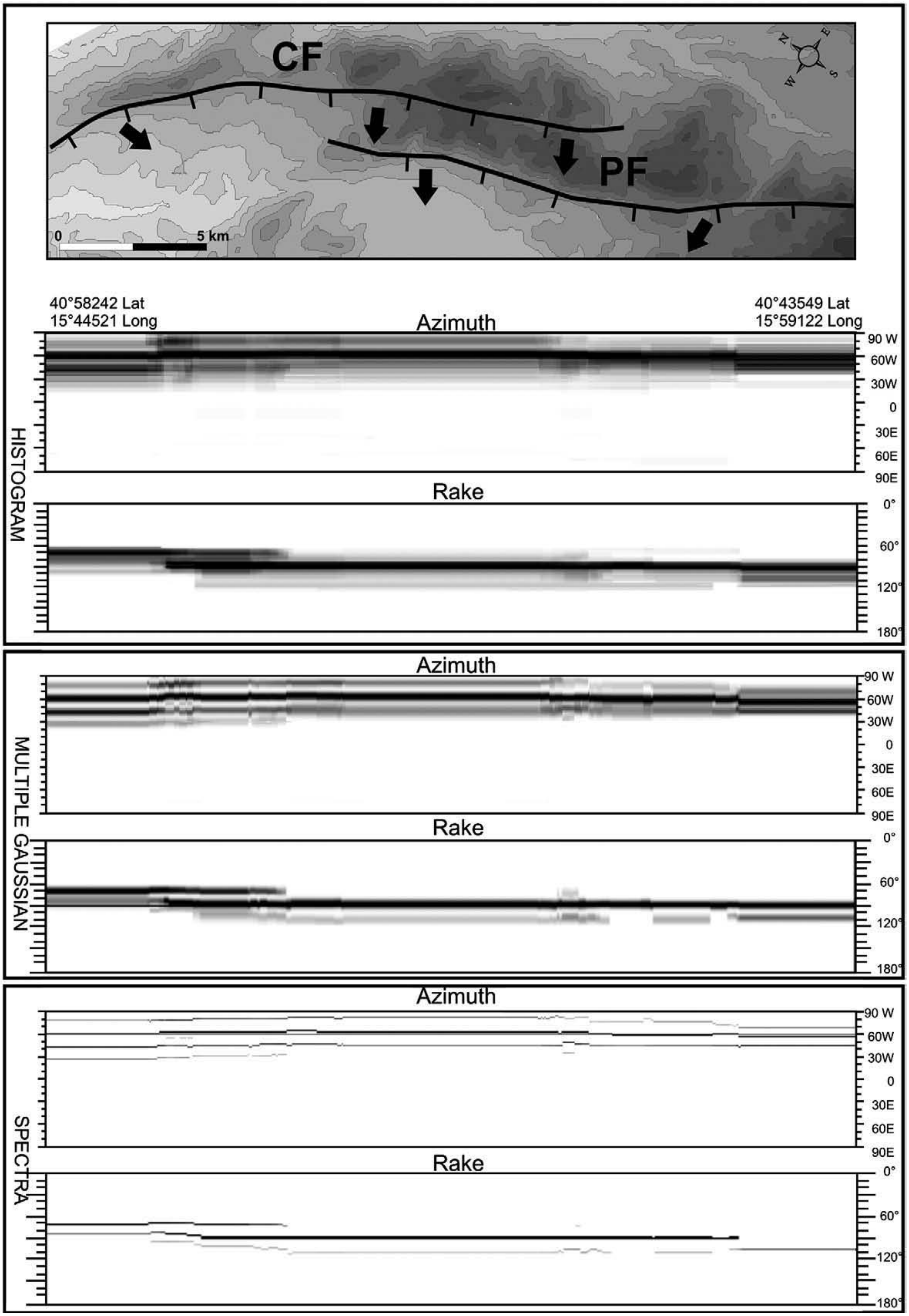

Fig. 6. Azimuthal distribution and pitch variation along the strike of the mapped active faults. This analysis has been carried out with Daisy 3, a Structural Data Integrated System Analiser, developped by Salvini F. and available at the following web site: http://host.uniroma3.it/progetti/fralab/Downloads/Programs/.

Please cite this article as: Spina, V., et al., Quaternary fault segmentation and interaction in the epicentral area of the 1561 earthquake (Mw = 6.4), Vallo di Diano, southern Apennines, Italy, Tectonophysics (2008), doi:10.1016/j.tecto.2007.06.012

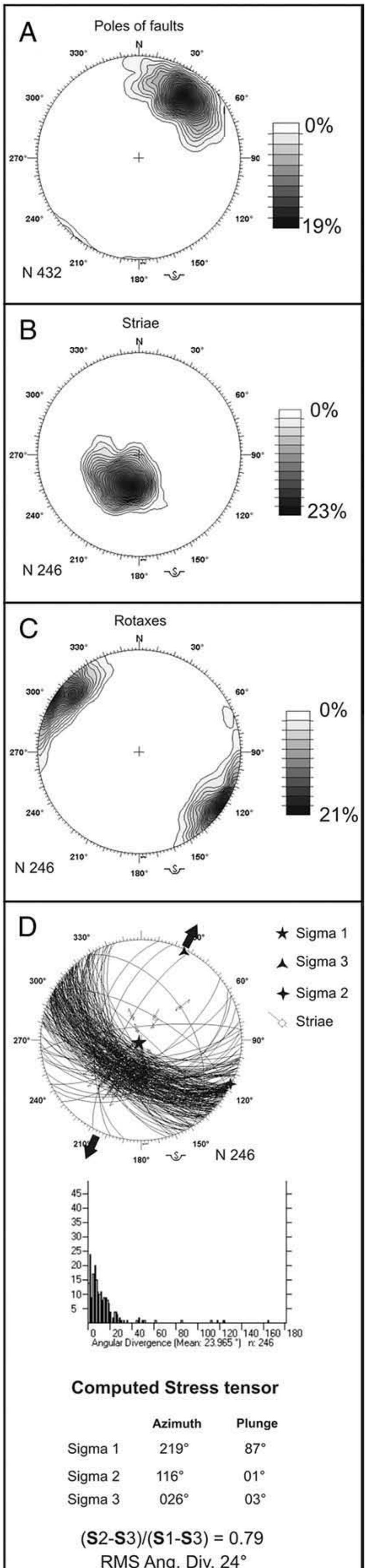

Fig. 7. Structural data. (A) Contour diagram of poles of the fault planes. (B) Contour diagram of striae directions measured along the fault surfaces. (C) Contour diagram of rotaxes. (D) Stress tensor geometry, obtained from slip data collected along the two analysed faults, using Angelier's inversion method (Daisy software; http://host.uniroma3.it/progetti/fralab/Downloads/Programs/).

2003; Galli et al., 2006). For most of the exposed fault trace, it brings into contact Mesozoic carbonate and Miocene flysch units with Quaternary slope breccias; at its southern termination, it cuts through Middle Pleistocene slope deposits (Fig. 4). The geomorphic signature of the CF is given by a 3–6 m high fault scarp in the northern sector (Fig. 4) developed within carbonates. In the southern sector, the fault zone displays a segmented pattern, with fault scarps arranged *en echelon* and bordering the intermountain basins filled with upper Pleistocene alluvial–colluvial deposits (Fig. 4). Fault rocks, represented by breccia and gouge have a thickness ranging between a few millimeters and 15 cm, in the hanging wall, and between a few millimeters and 8 cm in the footwall (see also Cello et al., 2001a,b).

The Polla Fault (PF) is a 13 km-long structure exposed along the western foothill of the Monti della Maddalena Ridge. This fault cuts and back tilts Middle Pleistocene slope deposits (Ascione et al., 1992) cropping out near the Polla village (Fig. 5), and Late Pleistocene slope deposits (according to Cello et al., 2003) exposed at its southern termination. Fresh fault scarps may be observed all along its length, which consist of smoothed and striated fault surfaces and of breccia and gouge with a thickness varying between a few millimetres and 7 cm.

The overlap (O) between the CF and PF is almost 7 km, whereas the separation (S) is around 3 km; hence the ratio O/S ~ 2.3.

In the Vallo di Diano area, we performed detailed geological mapping (at the scale of 1:10,000) and a systematic structural study that include: (i) fault orientation analysis, (ii) displacement–length profiling, and (iii) kinematic indicator analysis. The above data were then re-assessed using the *Transect Analysis* method (Salvini et al., 1999). This statistical method includes three progressive steps: Histogram Analysis, Multiple Gaussian Analysis, and Spectral Analysis. By applying this methods, it is possible to filter the distribution and frequency data of the selected parameters. Histogram Analysis allows the obtaining frequency-histograms plotted along a transect parallel to the fault trace. Multiple Gaussian and Spectral Analyses allows the definition of the shape of the Gaussian wave and of the Gaussian peak along the same transect.

4.1. Transect Analysis

Transect Analysis of the CF and PF assess the azimuthal distribution and pitch variations of fault-related mesostructures along the fault-parallel transects. The diagrams in Fig. 6 show that the trend of the main fault-related mesofaults is roughly NW–SE in the external fault tip areas, whereas in the overlap zone the mesoscale structures exhibit a mainly WNW–ESE orientation. The pitch distribution of striations also appears to be site-dependent (Roberts and Ganas, 2000; Roberts et al., 2004): at the northern tip zone, the mean pitch value is about 65° (hence indicating that here oblique left-lateral motion is dominant), whereas at the southern termination the pitch value ranges between 90° and 120° (indicating a right-lateral component of the motion). In the central sector, we recorded pitch values close to 90° (indicating a pure dip–slip motion).

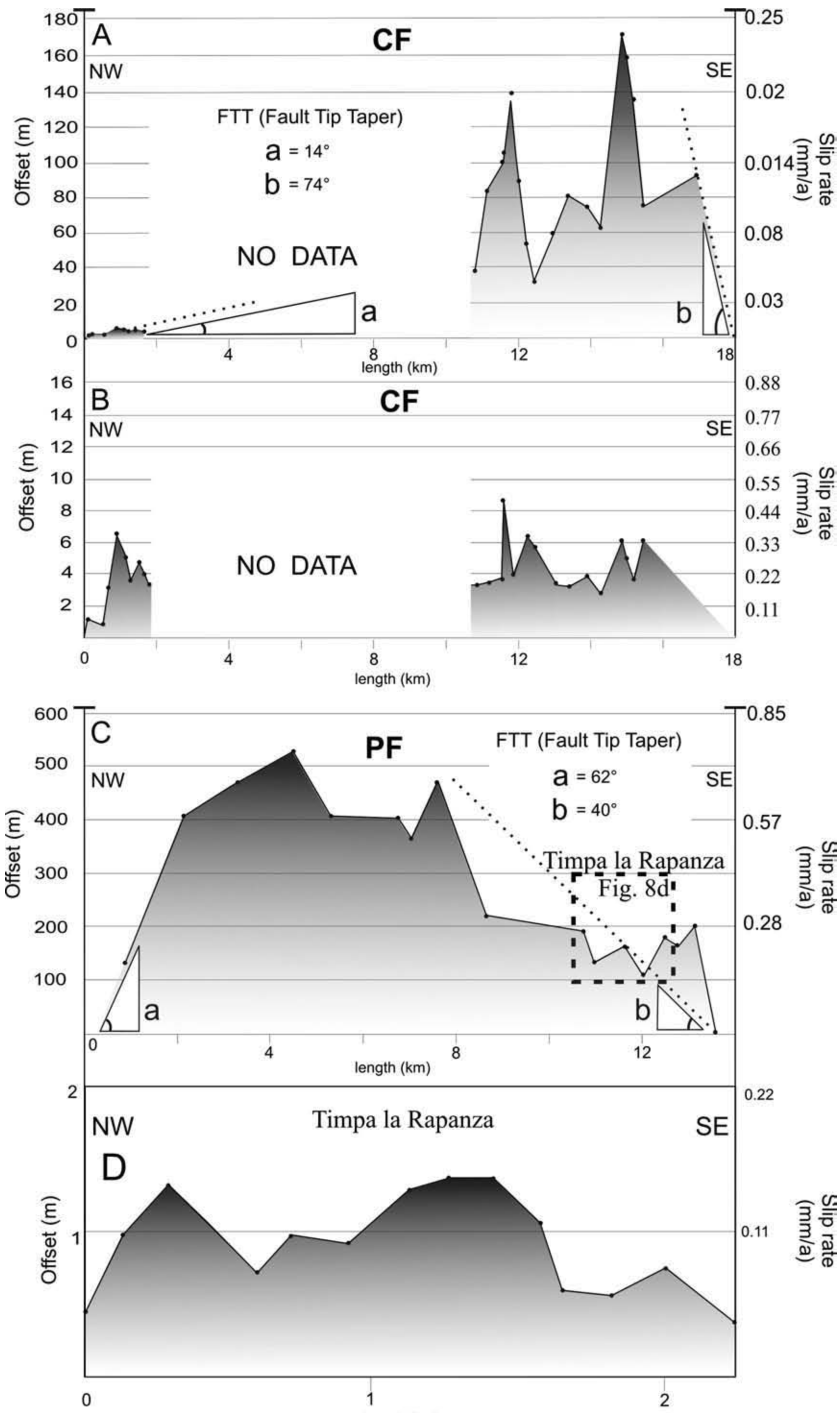

Fig. 8. Length–displacement profiles obtained from morphological offsets (represented by the height of the fault scarps), which were measured using topographic profiles across the fault scarps. (A) Diagram related to the long-term (since Middle Pleistocene times, according to Cello et al., 2003 and Galli et al., 2006) tectonic activity of the CF. The strong complexity shown by the several spites in the diagram can be related to shallow fault segmentation. Note that the angles between the tangent to the profiles and the horizontal computed at the northern and southern tip zones (FTT angles, Scholz and Gupta, 2000) show different values. (B) Diagram representative of the post last-glacial peak (18 ka) tectonic activity of the CF. (C) Diagram related to the long-term (since Middle Pleistocene times, according to Ascione et al., 1992; Cello et al., 2003; Galli et al., 2006) tectonic activity of the PF. The throw distribution shows that the highest values are concentrated in the northernmost sector of the fault. As for the CF fault, the FTT angles show different values. (D) Diagram of the southern fault scarp related to the post last-glacial peak reactivation of the PF.

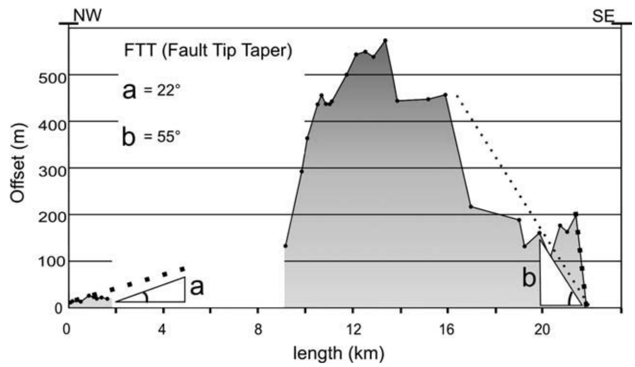

Fig. 9. Cumulative length–displacement profile relative to both faults, the CF and the PF. Note that the FTT angles show very different values, indicating a possible interaction of the Vallo di Diano Fault System (including CF and PF) with the Val d'Agri Fault System (see also Cello et al., 2003).

The results of stress inversion, which is based on measured fault planes and striae, as well as rotaxes are shown in Fig. 7. This permitted us to reconstruct the stress field geometry and the stress axial ratio (R) of the stress ellipsoid acting in the area. In particular, the rotaxes (rotational axes, *sensu* Wise & Vincent, 1965) represent structural lineations on fault planes orthogonal to the slip vector (corresponding to the direction of the maximum shear stress). When a conjugate set of faults develops, rotaxes are the only structural elements which keep exactly the same orientation. Because their clustering on a stereogram indicate the intermediate axis of the stress ellipsoid ($\sigma 2$), it is thus possible to differentiate many tectonic phases or deformations events based on the occurrence of more clusters.

4.2. Length–displacement profiles

Based on the results of our field mapping, we constructed several geological profiles across the Vallo di Diano basin; this allowed us to estimate the offset of significant geological markers. One of such markers is the unconformable contact, formed prior to the extension, of the Miocene flysch units with the Apenninic carbonate rock units below. The cumulative offset of this contact, as measured from geological profiles, is consistent with the geomorphological offset (represented by the height of the fault scarps), which were measured using topographic profiles across the fault scarps. This means that it is reasonable to use the geomorphological offset to build up appropriate length–displacement diagrams (Figs. 8A and C).

At the base of the CF scarp we recognized a steep and smooth fault surface involving 16Ka slope deposits, which are younger than the last glacial peak (18 ka old, Galli et al., 2006). We also observed faulted deposits of Late Pleistocene or Holocene age (according to Cello et al., 2003) along the southernmost sector of the PF at the Timpa la Rapanza (see also Fig. 4D in Cello et al., 2003). Those deposits are similar, in terms of stratigraphic position, to the faulted soils dated 20–40 ka and described by Giano et al. (2000) in the Val d'Agri area. Based on the above information, we consider the morphological break exposed at the base of both the CF and PF scarps as the result of fault slip after the Last Glacial Maximum (almost 18 ka, see Fig. 8B and D).

In Fig. 8A and C, it is also possible to observe that the length–displacement profiles of the long-term activity (since

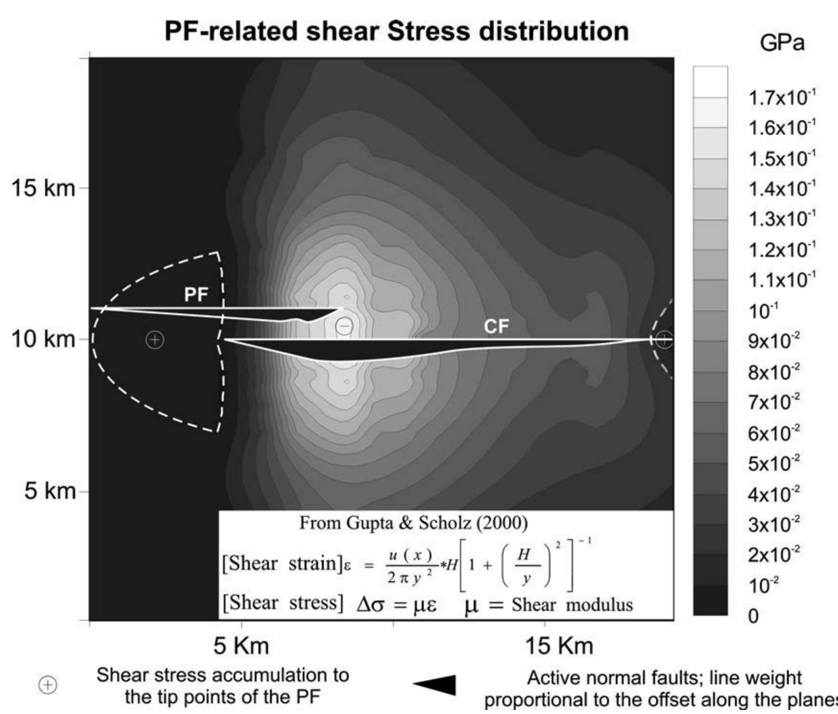

Fig. 10. Shear stress has been modelled referring to the PF, using the theoretical model proposed by Gupta & Scholz (2000). As foreseen by the model, the offset-related stress decrease is related to the elastic deformation; in this way, a shear stress accumulation characterizes the tip points of the PF, allowing the lateral propagation of the northernmost tip point of the CF. Meanwhile, the southernmost tip point of the CF, falls in the most intense shear stress drop area, where propagation is inibithed and offset accumulations is enanched. In the figure, lines weight shows how the offset anomalies are concentrated in the overlap region of the two faults.

Please cite this article as: Spina, V., et al., Quaternary fault segmentation and interaction in the epicentral area of the 1561 earthquake (Mw = 6.4), Vallo di Diano, southern Apennines, Italy, Tectonophysics (2008), doi:10.1016/j.tecto.2007.06.012

Middle Pleistocene times, according to Ascione et al., 1992; Cello et al., 2003; Galli et al., 2006) of the CF and the PF faults, are asymmetric. In fact, the angles between the tangent to the profiles and the horizontal (FTT angles, Scholz and Gupta, 2000) computed at the northern and southern tip zones of each faults show different values. Furthermore, using the cumulative displacement for both faults, a throw/length ratio (γ) of 0.01 is obtained for the CF, whereas a γ value of 0.04 characterises the PF. Moreover, the cumulative length–displacement profiles computed for both faults (Fig. 9) shows different value of the tangent angles (FTT) indicating a possible interaction with the Val d'Agri Fault System, as suggested by Cello et al. (2003).

4.3. Structural interpretation and Coulomb stress analysis

Following Galli et al. (2006, for the CF) and Cello et al. (2003, for both CF and PF), we infer that the two parallel faults (CF and PF), bounding the eastern side of the Vallo di Diano basin, are both active, because they locally offset very young slope deposits. The structural characterization of the CF and the PF suggests that, from a kinematics point of view, these faults may behave as a single structure (Roberts and Ganas, 2000; Roberts et al., 2004). The resulting length–displacement profiles are representative of both long-term (since Middle Pleistocene times, according to Ascione et al., 1992; Cello et al., 2003 and Galli et al., 2006) and short-term tectonic activities (since 18 ka) of both CF and PF. The length–displacement diagram resulting from the CF long-term tectonic activity (Fig. 8A) shows an eterogeneous pattern. We interpret this pattern as the evidence of an unconnected growing array of lower-rank fault segments (in the Early–Middle Pleistocene). On the other hand, the length-displacement diagram resulting from the long-term tectonic activity of the PF exhibits a more homogeneous shape, showing a maximum in the northern sector of the fault (Fig. 8C). Although both the CF and the PF show a clear morphological evidence of a recent tectonic activity, it should be noted that geological evidences of active deformation during the Holocene are found mainly along the CF (Cello et al., 2003; Galli et al., 2006) and at the southern termination of the PF (Cello et al., 2003).

The length–displacement profile constructed across individual faults show a marked asymmetry (see Fig. 8). In fact, at the tip points, the angles between the tangent to the profiles and the horizontal (FTT angles), are quite different. Following Scholz and Gupta (2000), we suggest that this geometric property is indicative of the strong interaction between the two analysed faults. The shear stress drop, due to fault motion, generates an energetic barrier that restricts fault lateral growth (Fig. 10). In the case of the CF and PF, we suggest that the shear stress distribution related to the long-term tectonic activity of both faults is such that it favours offset accumulation in the stress shadow area, hence producing a distorted length–displacement profile in the overlapping zone. The above information is consistent with the following statement. Within the structural context of this sector of the Apennines, any earthquake event associated with one of the two faults may impose positive increments to the local stress state and hence enhance an almost simultaneous release of seismic energy by rupture processes on nearby along-strike seismogenic faults, generating larger earthquakes (Cowie, 1998).

In order to model the positive or negative variations of the local stress state, we computed the Coulomb stress changes due to the activation of the CF by using the GNstress software (Robinson, 2002). The geometric parameters used for computation are listed in Table 1, and are based on our field observations. Using the Wells & Coppersmith (1994) relations we also inferred the average displacement and the seismic potential of the CF (M ~ 6.5, see also Tondi, 2000 and Galli et al., 2006). Other parameters needed for the computation are shown in Table 2. In our model the fault is considered to be an inclined (65°) rectangular surface with the longer side corresponding to the fault length (17 km) and the shorter side set by the depth of the seismogenic crust (15 km). In order to take into account the kinematic complexity of the structure (i.e. pitch variations and slip distribution), the CF has been subdivided into five cells (Fig. 11). The first one, corresponding to the northernmost section of the fault, is characterized by an oblique left-lateral component of motion, whereas the last cell, corresponding to its southern termination, is characterized by a

Table 1
Dimensional parameters representative of the CF

CF length=15 km	Strike N130E°	CF dip=65°
Wells & Coppersmith (1994)	Log (D)=−1.43+0.88*Log(L) M=5.08+1.16*Log(L)	D=0.4 M=6.5

The average displacement (D=0.4, in metres) and the seismic potential (M=magnitude) of the fault are inferred from the empirical relationships proposed by Wells & Coppersmith (1994).

Table 2
Input parameters in the GnStress 2.17 (Robinson, 2002)

Friction coefficient	Poisson ratio
0.7	0.25
Pore Pressure (λ_c)	Rigidity (Nm^{-2})
0.38	2.68
Skempton's coefficient	Density (g/cm^3)
0.5	2.65

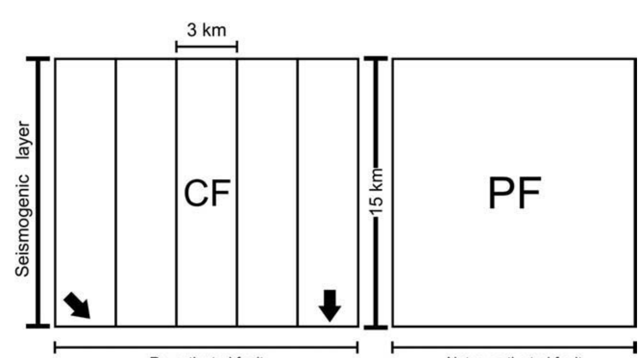

Fig. 11. Conceptual model of a rectangular surface approaching a fault. In order to keep into account the different pitch distributions, we sub-divided the CF in an almost 3 Km long rectangular cells.

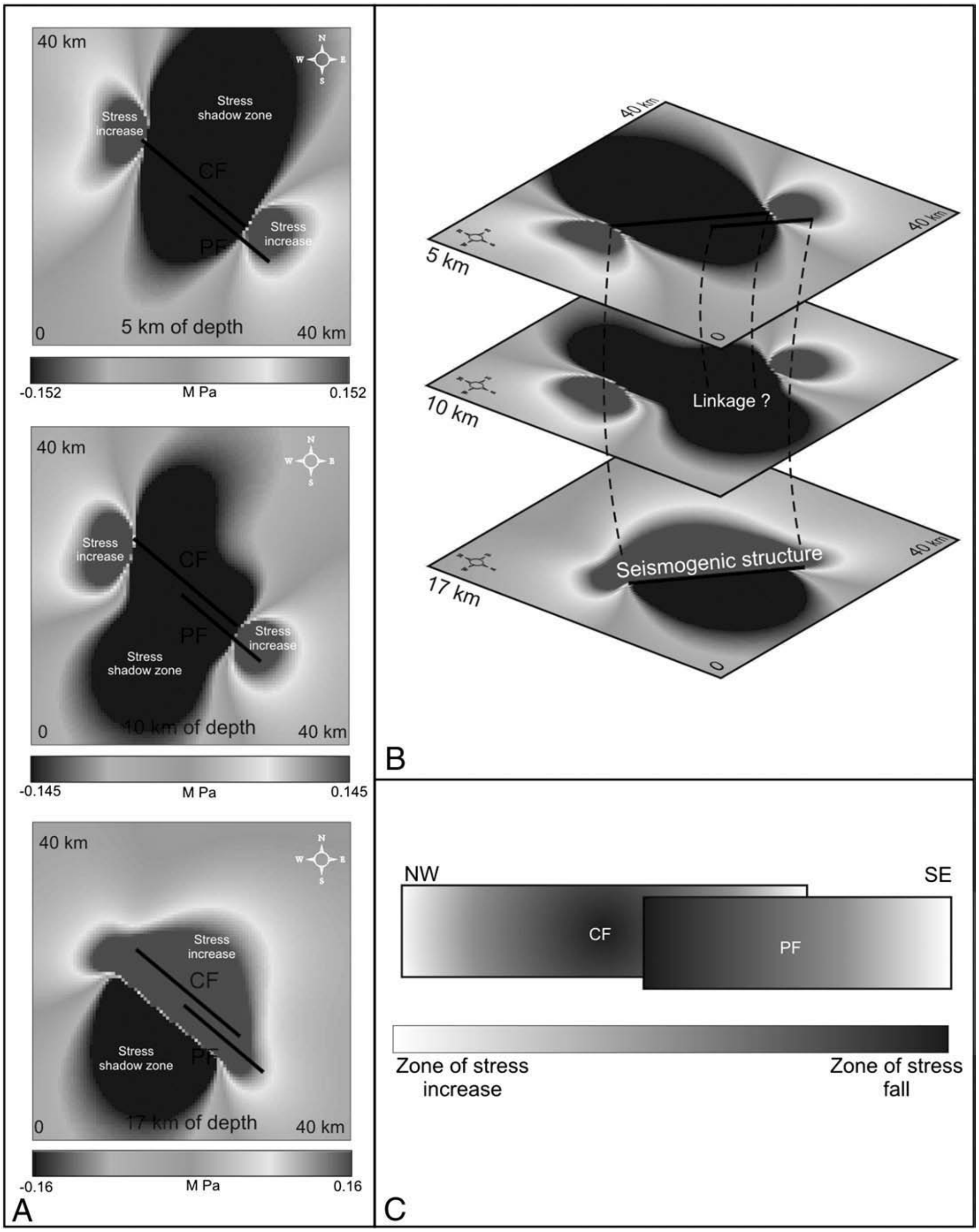

Fig. 12. Coulomb Stress changes along the CF. (A) Maps and (B) Block diagram showing co-seismic Coulomb stress distribution and possible fault geometry at depth. (C) Conceptual patterns of the co-seismic Coulomb stress distribution along each fault due to CF re-activation. This produces a large stress drop along almost the entire CF plane, with two stress increase zones concentrated at the tip points. This scenario determines a stress drop along the PF, but a stress loading of its southernmost part. This part of the fault can be re-activated because stress triggering in occasion of the 1561 earthquake.

dip–slip (normal) motion. We assume a vertical co-seismic displacement of 0.40 m, which is consistent with the results of recent palaeoseismological investigations (Galli et al., 2006).

The software used to compute Coulomb stress changes (CFS) within a half-space model expresses those variations as:

$$\delta CFS = \delta T_{\text{shear}} + \mu(\delta T_n + \delta P) \quad (1)$$

where μ is the coefficient of dry friction, $\delta\tau_{\text{shear}}$ is the induced change in shear stress, $\delta\tau_{\text{n}}$ is the induced change in normal stress, and δP is the induced change in pore pressure. The latter is given by:

$$\delta P = (\beta/3)\sum \delta T_{ii} \quad (2)$$

where β is Skempton's coefficient (for details, see also Harris, 1998; Okada, 1992; King and Cocco; 2001; Steacy et al., 2005).

Assuming that the fault is optimally oriented for re-shear with respect to the remote stress field, and that it reactivates for its entire length, the resulting CFS distribution on flat surfaces at 5, 10 and 15 km depth is shown in Fig. 12. Reactivation of the CF induces two zones of stress accumulation at depths of 5 and 10 km, which are localized at the northern and southern fault tip areas. However, at 15 km depth a stress-increasing zone develops in the footwall of the CF. This almost continuous front of stress accumulation is not different from that induced by a single fault extending laterally for about 20 km. On the other hand, reactivation of the CF is also responsible for the development of a stress shadow area in the overlap zone. This latter process could be, in our opinion, the major factor inhibiting seismic energy release, as also suggested by the lack of geological evidence of active deformation in this sector of the PF.

5. Conclusions

Integrated structural and morphotectonic analyses were carried out on the fault zones bounding the eastern side of the Vallo di Diano tectonic depression, in southern Italy. The analysed structures include two active fault segments: the Caggiano Fault (CF) and the Polla Fault (PF). Our study outlines the following main features:

1) Although forming separate fault segments, the CF and PF are characterized by space-dependent slip variations that are consistent with a changing kinematic behaviour towards a single structure (see also Roberts and Ganas, 2000).
2) The length–displacement profile for each fault segment shows a significant asymmetry, suggesting that the long-term activity was strongly influenced by interaction processes in the overlap zone between the two faults (see also Gupta & Scholz, 2000).
3) The fault slip distribution is consistent with the two active segments being part of a single fault zone.
4) Activation of the CF may generate $M = 6.5$ earthquakes (i.e. the 1561 earthquake, Mw = 6.4). The Coulomb Stress Changes due to any event of this size indicate that the co-seismic stress drops in the hanging wall of the CF would tend to inhibit further activity along the PF, except for its southern termination.

Acknowledgements

Professors G.P. Roberts and A.M. Michetti strongly improved the manuscript. Professor S. Critelli is thanked for discussions and the support during field work.

Finally, V. Spina is indebted to Dr. Mauro Alessandroni for the assistance.

References

Ascione, A., Cinque, A., Santangelo, N., Tozzi, M., 1992. Il bacino del Vallo di Diano e la tettonica trascorrente plio-quaternaria: nuovi vincoli cronologici e cinematici. Studi Geologici Camerti 209–220 Special Issue.

Benedetti, L., Tapponier, P., King, G.C.P., Piccardi, L., 1998. Surface rupture of the 1857 Southern Italian earthquake. Terra Nova 10 (4), 206–210.

Boschi, E., Guidoboni, E., Ferrari, G., Valensise, G., Gasperini, P. (Eds.), 1997. Catalogo dei forti terremoti in Italia dal 461 a.C. al 1990, vol. 2. ING-SGA, Bologna, p. 644.

Branno, A., Esposito, E., Maturano, A., Porfido, S., Rinaldis, V., 1983. Studio, su base macrosismica, del terremoto della Basilicata del 16 dicembre 1857. Bollettino della Società dei Naturalisti di Napoli, XCII, p. 338.

Butler, R.W.H., Mazzoli, S., Corrado, S., De Donatis, M., Di Bucci, D., Gambini, R., Naso, G., Nicolai, C., Scrocca, D., Shiner, P., Zucconi, V., 2004. Applying thick-skinned tectonic models to the Apennine thrust belt of Italy: Limitations and implications. In: McClay, K.R. (Ed.), Thrust Tectonics and Petroleum Systems. vol. 82. American Association of Petroleum Geologists Memoir, pp. 647–667.

Cartwright, J.A., Trudgill, B.D., Mansfeld, C.S., 1995. Fault growth by segment linkage: an explanation for scatter in maximum displacement and trace length data from the Canyonlands Grabens of SE Utah. Journal of Structural Geology 17, 1319–1326.

Catalano, S., Monaco, C., Tortorici, L., Paltrinieri, W., Steel, N., 2004. Neogene–Quaternary evolution of the southern Apennines. Tectonics 23, TC2003, 1–19.

Cello, G., Mazzoli, S., 1999. Apennine tectonics in southern Italy: a review. Journal of Geodynamics 27, 191–211.

Cello, G., Guerra, I., Tortorici, L., Turco, E., Scarpa, R., 1982. Geometry of the neotectonic stress field in southern Italy: geological and seismological evidence. Journal of Structural Geology 4, 385–393.

Cello, G., Martini, N., Paltrinieri, W., Tortorici, L., 1989. Structural styles in the frontal zones of the southern Apennines, Italy: an example from the Molise district. Tectonics 8 (4), 753–768.

Cello, G., Mazzoli, S., Tondi, E., Turco, E., 1997. Active tectonics in the Central Apennines and possible implications for seismic hazard analysis in peninsular Italy. Tectonophysics 272, 43–68.

Cello, G., Tondi, E., Micarelli, L., Invernizzi, C., 2001a. Fault zone fabrics and geofluid properties as indicators of rock deformation modes. Journal of Geodynamics 32, 543–565.

Cello, G., Invernizzi, C., Mazzoli, S., Tondi, E., 2001b. Fault properties and fluid flow patterns from Quaternary faults in the Apennines, Italy. Tectonophysics 336 (1–4), 63–78.

Cello, G., Tondi, E., Micarelli, L., Mattioni, L., 2003. Active tectonics and earthquake sources in the epicentral area of the 1857 Basilicata earthquake (Southern Italy). Journal of Geodynamics 36, 37–50.

Cinque, A., Patacca, E., Scandone, P., Tozzi, M., 1993. Quaternary kinematic evolution of the Southern Apennines. Relationships between surface geological features and deep lithospheric structures. Annali di Geofisica 36, 249–260.

Cowie, P.A., 1998. A healing–reloading feedback control on the growth rate of seismogenic faults. Journal of Structural Geology 20, 1075–1087.

Cowie, P.A., Roberts, G.P., 2001. Constraining slip rates and spacings for active normal faults. Journal of Structural Geology 23, 1901–1915.

D'Argenio, B., Pescatore, T., Scandone, P., 1973. Schema geologico dell'Appennino meridionale. Atti dell' Accademia Nazionale dei Lincei 183, 49–72.

Dewey, J.F., Helman, M.L., Turco, E., Hutton, D.H.W., Knott, S.D., 1989. Kinematics of the western Mediterranean. In: Coward, M.P., Dietrich, D., Park, R.G. (Eds.), Alpine Tectonics: Geological Society of London Special Publication, vol. 45, pp. 265–283.

Galadini, F., Galli, P., 2000. Active tectonics in the central Apennines(Italy). Input data for seismic hazard assessment. Natural Hazards 22, 202–223.

Galli, P., Bosi, V., 2003. Analisi paleosismologiche lungo la faglia di Caggiano (Monti della Maddalena, SA). Abstract GNGTS 2003.

Galli, P., Bosi, V., Piscitelli, S., Giocoli, A., Scionti, V., 2006. Late Holocene earthquakes in southern Apennine: paleoseismology of the Caggiano fault. Int. J. Earth Sci. doi:10.1007/s00531-005-0066-2 (Geol Rundsch).

Giano, S.I., Maschio, L., Alessio, M., Ferranti, L., Improta, S., Schiattarella, M., 2000. Radiocarbon dating of active faulting in the Agri high valley, southern Italy. Journal of Geodynamics 29, 371–386.

Gupta, A., Scholz, C.H., 2000. A model of normal fault interaction based on observations and theory. Journal of Structural Geology 22, 865–879.

Harris, R.A., 1998. Introduction to special section: stress triggers, stress shadows, and implications for seismic hazard. Journal of Geophysical Research 103, 24,347–24,358.

Hippolyte, J.-C., Angelier, J., Roure, F., Casero, P., 1994. Piggyback basin development and thrust belt evolution: structural and palaeostress analyses

Please cite this article as: Spina, V., et al., Quaternary fault segmentation and interaction in the epicentral area of the 1561 earthquake (Mw = 6.4), Vallo di Diano, southern Apennines, Italy, Tectonophysics (2008), doi:10.1016/j.tecto.2007.06.012

of Plio-Quaternary basins in the Southern Apennines. Journal of Structural Geology 16, 159–173.

Hodgkinson, K.M., Stein, R.S., King, G.C.P., 1996. The 1954 Rainbow Mountain–Fairview Peak–Dixie Valley earthquakes: a triggered normal faulting sequence. Journal of Geophysical Research 101, 25459–25471.

Kastens, K., Mascle, J., Auroux, C., Bonatti, E., Broglia, C., Channell, J.E.T., Curzi, P., Kay-Christian, E., Glacon, G., Hasegawa, S., Hieke, W., Mascle, J., McCoy, F., McKenzie, J., Mendelson, J., Muller, C., Rehault, J.-P., Robertson, A., Sartori, R., Sprovieri, R., Torii, M., 1988. ODP Leg 107 in the Tyrrhenian Sea: Insights into passive margin and back-arc basin evolution. Geological Society of America Bulletin 100, 1140–1156.

King, G., Cocco, M., 2001. Fault interaction by elastic stress changes: New clues from earthquake sequences. Advances in Geophysics 44, 1–38.

Mazzoli, S., Helman, M., 1994. Neogene patterns of relative motion for Africa–Europe: some implications for recent central Mediterranean tectonics. Geologische Rundschau 83, 464–468.

Mazzoli, S., Barkham, S., Cello, G., Gambini, R., Mattioni, L., Shiner, P., Tondi, E., 2001. Reconstruction of continental margin architecture deformed by the contraction of the Lagonegro Basin, Southern Apennines, Italy. Geological Society of London Journal 158, 309–319.

Montone, P., Amato, A., Pondrelli, S., 1999. Active Stress Map of Italy. Journal of Geophysical Research 104 (B11), 25,595–25,610.

Mostardini, F., Merlini, S., 1986. Appennino centro-meridionale. Sezioni geologiche e proposta di modello strutturale. Memorie della Società Geologica Italiana 35, 177–202.

Okada, Y., 1992. Internal deformation due to shear and tensile faults in a half-space. Bulletin of the Seismological Society of America 82, 1018–1040.

Pantosti, D., Valensise, G., 1990. Faulting mechanism and complexity of the 23 November 1980, Campania–Lucania earthquake, inferred from surface observations. Journal of Geophysical Research 95, 15319–15341.

Peacock, D.C.P., Sanderson, D.J., 1991. Displacements, segment linkage and relay ramps in normal fault zones. Journal of Structural Geology 13, 721–733.

Porfido, S., Esposito, E., Vittori, E., Tranfaglia, G., Michetti, A.M., Blumetti, A.M., Ferreli, L., Guerrieri, L., Serva, L., 2002. Areal distribution of round effects induced by strong earthquakes in the southern Apennines (Italy). Surveys in Geophysics 23, 529–562.

Roberts, G.P., Cowie, P., Papanikolaou, I., Michetti, A.M., 2004. Fault scaling relationships, deformation rates and seismic hazard: an example from the Lazio–Abruzzo Apennines, central Italy. Journal of Structural Geology 26, 377–398.

Roberts, G.P., Ganas, A., 2000. Fault–slip directions in central-southern Greece measured from striated and corrugated fault planes: comparison with focal mechanism and geodetic data. Journal of Geophysical Research 105, 23,443–23,462.

Robinson, R., 2002. GnStress_2: A Computer Programme for Inverting First Motion Observations to a Regional Stress Tensor. Institute of Geological & Nuclear Sciences Box 30368, Lower Hutt, New Zealand.

Rosenbaum, G., Lister, G.S., Duboz, C., 2002. Relative motions of Africa, Iberia and Europe during Alpine orogeny. Tectonophysics 359, 117–129.

Salvini, F., Billi, A., Wise, D.U., 1999. Strike–slip fault-propagation cleavage in carbonate rocks: the Mattinata Fault Zone, Southern Apennines, Italy. Journal of Structural Geology 21, 1731–1749.

Scandone, P., Bonardi, G., 1968. Synsedimentary tectonic controlling of Mesozoic and Tertiary carbonate sequence of areas sourrounding Vallo di Diano. Memorie della Società Geologica Italiana 7, 1–10.

Scholz, C.H., Gupta, A., 2000. Fault interactions and seismic hazard. In: Cello, G., Tondi, E. (Eds.), The resolution of geological analysis and models for earthquake faulting studies. Journal of Geodynamics, vol. 29(3–5), pp. 317–323.

Sgrosso, I., 1998. Possibile evoluzione cinematica miocenica nell'orogene centro-sud appenninico. Bollettino della Società Geologica Italiana 117, 679–724.

Steacy, S., Gomberg, J., Cocco, M., 2005. Introduction to special section: Stress transfer, earthquake triggering, and time-dependent seismic hazard. Journal of Geophysical Research 110, B05S01. doi:10.1029/2005JB003692.

Tondi, E., 2000. Geological analysis and seismic hazard in the Central Apennines. In: Cello, G., Tondi, E. (Eds.), The resolution of geological analysis and models for earthquake faulting studies. Journal of Geodynamics, vol. 29 (3–5), pp. 517–534.

Willemse, E.J.M., Pollard, D.D., Aydin, A., 1996. Three-dimensional analyses of slip distributions on normal fault arrays with consequences for fault scaling. Journal of Structural Geology 18, 295–909 Nos 2/3.

Willemse, E.J.M., 1997. Segmented normal faults: correspondence between three dimensional mechanical models and field data. Journal of Geophysical Research 102, 675–692.

Wise, D.U., Vincent, R.J., 1965. Rotation axis method for detecting conjugate planes in calcite petrofabric. American Journal of Science 263, 289–301.

Wells, D.L., Coppersmith, K.J., 1994. New empirical relationships among magnitude, rupture length, rupture width, rupture area, and surface displacement. Bulletin of Seismological Society of America 84, 974–1002.

Working Group CPTI, 2004. Catalogo Parametrico Terremoti Italiani, ING, GNDT, SGA, SSN, 92 pp., Bologna.

Please cite this article as: Spina, V., et al., Quaternary fault segmentation and interaction in the epicentral area of the 1561 earthquake (Mw = 6.4), Vallo di Diano, southern Apennines, Italy, Tectonophysics (2008), doi:10.1016/j.tecto.2007.06.012